

The Channel Multivariate Entropy Triangle and Balance Equation

Francisco J. Valverde-Albacete, *Member, IEEE*, and Carmen Peláez-Moreno, *Member, IEEE*

Abstract

In this paper we use information-theoretic measures to provide a theory and tools to analyze the flow of information from a discrete, multivariate source of information \bar{X} to a discrete, multivariate sink of information \bar{Y} joined by a distribution $P_{\bar{X}\bar{Y}}$. The first contribution is a decomposition of the maximal potential entropy of (\bar{X}, \bar{Y}) that we call a *balance equation*, that can also be split into decompositions for the entropies of \bar{X} and \bar{Y} respectively. Such balance equations accept normalizations that allow them to be represented in de Finetti entropy diagrams, our second contribution. The most important of these, the aggregate Channel Multivariate Entropy Triangle CMET is an exploratory tool to assess the efficiency of multivariate channels. We also present a practical contribution in the application of these balance equations and diagrams to the assessment of information transfer efficiency for PCA and ICA as feature transformation and selection procedures in machine learning applications.

Index Terms

Entropy, Entropy visualization, Entropy balance equation, Shannon-type relations, Multivariate analysis, Machine Learning Assessment, Data transformation evaluation.

I. INTRODUCTION AND MOTIVATION

Information-related considerations are often cursorily invoked in many machine learning applications sometimes to suggest why a system or procedure is seemingly better than another at a particular task. In this paper we set out to ground on measurable evidence phrases such as “this transformation retains more information from the data” or “this learning method uses better the information from the data than this other.”

To fix notation, let $\bar{X} = \{X_i \mid 1 \leq i \leq n\}$ be a set of discrete random variables with joint multivariate distribution $P_{\bar{X}} = P_{X_1 \dots X_n}$, and the corresponding marginals $P_{X_i}(x_i) = \sum_{j \neq i} P_{\bar{X}}(\bar{x})$ where $\bar{x} = x_1 \dots x_n$ is a tuple of n elements. And likewise for $\bar{Y} = \{Y_j \mid 1 \leq j \leq l\}$, with $P_{\bar{Y}} = P_{Y_1 \dots Y_l}$ and the marginals P_{Y_j} . Furthermore let $P_{\bar{X}\bar{Y}}$ be the joint distribution of the $(n + l)$ -length tuples $\bar{X}\bar{Y}$.

In many applications, \bar{X} carries a prior information and $\bar{Y} = f(\bar{X})$ is derived from it. Our motivating application is the following: consider the block diagram in Figure 1 describing a data transformation over a data source and sink, where \bar{X} represents the original data and $\bar{Y} = f(\bar{X})$ the transformed data. For the purpose at hand it does

F.J. Valverde-Albacete and C. Peláez-Moreno are with the Department of Signal Theory and Communications, Universidad Carlos III de Madrid, Leganés 28911, Spain, e-mail: fva,carmen@tsc.uc3m.es

Manuscript received April 19, 2005; revised August 26, 2015.



Fig. 1. Transformation block implementing $\bar{Y} = f(\bar{X})$. \bar{X} is the data source and \bar{Y} the transformed data.

not matter what particular transformation is carried out in the block. Rather, we are interested in whether all of the “relevant” information extant in \bar{X} is transferred to \bar{Y} . This imposes a *net flow of information* “through” the distribution $P_{\bar{X}\bar{Y}}$ from \bar{X} , conceived as an *input*, to \bar{Y} , considered as an *output*¹.

This kind of block may represent, for instance, a PCA, ICA or any other unsupervised transformation method, in which case the “relevance” must be supplied by a heuristic principle, e.g. least reconstruction error on some test data, etc. But it may also represent a supervised transformation method—for instance, \bar{X} are the feature instances and \bar{Y} are the (multi)labels or classes in a classification task— \bar{Y} may be the activation signals of the convolutional neural network trained using an implicit target signal, in which case, the “relevance” is supplied by the conformance to the supervisory signal.

We will try to provide a solution to this problem using the relatively new framework of *entropy balance equations* and their related *entropy triangles*. For instance, it is well-proven that when $n = |\bar{X}| = |\bar{Y}| = l = 1$ we can evaluate the effectiveness of any “transformation” by measuring the transfer of information from single input to single output using the well-known measures dating back to Shannon but considering an extended relation between them in the form of a balance equation for their joint entropy [1],

$$H_{U_X \cdot U_Y} = \Delta H_{P_X \cdot P_Y} + 2 * MI_{P_{XY}} + VI_{P_{XY}} \quad (1)$$

$$0 \leq \Delta H_{P_X \cdot P_Y}, MI_{P_{XY}}, VI_{P_{XY}} \leq H_{U_X \cdot U_Y}$$

where U_X and U_Y are the uniform distributions on the supports of P_X and P_Y , respectively, and the information theoretic quantities are: a) the *divergence with respect to uniformity*, $\Delta H_{P_X \cdot P_Y}$, between the joint distribution where P_X and P_Y are independent and the uniform distributions with the same cardinality of events as P_X and P_Y , b) the *mutual information*, $MI_{P_{XY}}$ [2, 3], quantifying the strength of the stochastic binding between P_X and P_Y , and c) the *variation of information*, $VI_{P_{XY}}$ [4], that embodies the residual entropy not used in binding the variables. As an example application in machine learning, if X represents the class of some data samples and Y their predicted class in a multi-class classification task, we can information-theoretically assess the classifier that carried out the prediction [5]. Furthermore, this assessment can be carried out interactively in a flavor of Exploratory Data Analysis with a ternary plot diagram called the Channel Bivariate Entropy Triangle (CBET). We will briefly present the theory behind this case and some typical applications in Section II-A.

¹If we focus on the entropy transferred from any possible input to any possible output it is pertinent to call $P_{\bar{X}\bar{Y}}$ an INFORMATION CHANNEL. The capitals help here realize that we are considering a metaphor for the joint distribution. Some others may claim that the joint distribution is a MODEL for the channel, while the random vectors are MODELS for input and output.

But for multivariate input \bar{x} and output \bar{y} random vectors, in general, we need the multivariate generalizations of these information-theoretic measures $\Delta H_{P_X \cdot P_Y}$, $MI_{P_{XY}}$, and $VI_{P_{XY}}$, an issue that is not free of contention. With this purpose in mind, we review the best-known multivariate generalizations of mutual information in Section II-B.

In this paper we try and generalize this previous situation —single-input single-output (SISO) blocks $(X, Y) \sim P_{XY}$ —to a proper multivariate multiple-input multiple-output (MIMO) data transformation block described by its joint distribution $(\bar{X}, \bar{Y}) \sim P_{\bar{X}\bar{Y}}$. As a first result we develop a balance equation for the joint distribution $P_{\bar{X}\bar{Y}}$ and related representation in Sections III-A and III-B, respectively. But we are also able to obtain split equations for the input and output multivariate sources only tied by an analogue of mutual information, much as in the SISO case. Next as an instance of usage, in Section III-C we analyze the transfer of information in an instance of Principal Component Analysis and Independent Component Analysis applied to the well known Anderson’s iris dataset. We conclude with a discussion of the tools in light of this applications in Section III-D.

II. PRELIMINARIES

We will try to build a solution to our problem by finding the minimum common multiple, so to speak, of our previous solutions to the SISO block and the multivariate source cases, to be described next.

A. The Channel Bivariate Entropy Balance Equation and Triangle

A solution to conceptualizing and visualizing the transmission of information through a channel where input and output are reduced to a single variable, that is with $|\bar{X}| = 1$ and $|\bar{Y}| = 1$, was presented in [1] and later extended in [5]. For this case we use simply X and Y to describe the random variables and Figure 2.(a) depicts a classical information-diagram (i-diagram)[6, 7] of an entropy decomposition around P_{XY} to which we have included the exterior boundaries arising from *entropy balance equation* as we will show later. Three crucial regions can be observed:

- The *divergence with respect to uniformity*, $\Delta H_{P_X \cdot P_Y}$, between the joint distribution where P_X and P_Y are independent and the uniform distributions with the same cardinality of events as P_X and P_Y ,

$$\Delta H_{P_X \cdot P_Y} = H_{U_X \cdot U_Y} - H_{P_X \cdot P_Y}, \quad (2)$$

that shows how imbalanced the data and results are.

- The *mutual information*, $MI_{P_{XY}}$ [2, 3], quantifies the force of the stochastic binding between P_X and P_Y , “towards the outside”,

$$MI_{P_{XY}} = H_{P_X \cdot P_Y} - H_{P_{XY}} \quad (3)$$

but also “towards the inside”

$$MI_{P_{XY}} = H_{P_{\bar{X}}} - H_{P_{\bar{X}|\bar{Y}}} = H_{P_{\bar{Y}}} - H_{P_{\bar{Y}|\bar{X}}}. \quad (4)$$

- The *variation of information*, $VI_{P_{XY}}$ [4], embodies the residual entropy, not used in binding the variables,

$$VI_{P_{XY}} = H_{P_{X|Y}} + H_{P_{Y|X}}. \quad (5)$$

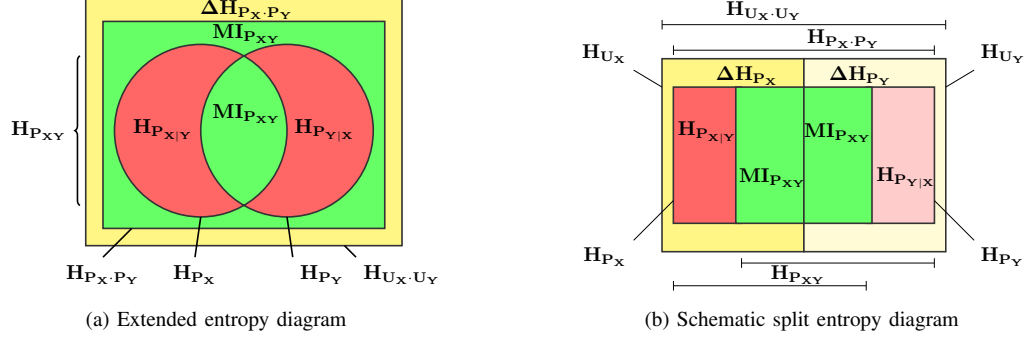


Fig. 2. Extended entropy diagram related to a bivariate distribution, from [1].

Then, we may write the following *entropy balance equation* between the entropies of X and Y :

$$H_{U_X \cdot U_Y} = \Delta H_{P_X \cdot P_Y} + 2 * MI_{P_{XY}} + VI_{P_{XY}} \quad (1, \text{revisited})$$

$$0 \leq \Delta H_{P_X \cdot P_Y}, MI_{P_{XY}}, VI_{P_{XY}} \leq H_{U_X \cdot U_Y}$$

where the bounds are easily obtained from distributional considerations [1]. If we normalize (1) by the overall entropy $H_{U_X \cdot U_Y}$ we obtain

$$1 = \Delta' H_{P_X \cdot P_Y} + 2 * MI'_{P_{XY}} + VI'_{P_{XY}} \quad 0 \leq \Delta' H_{P_X \cdot P_Y}, MI'_{P_{XY}}, VI'_{P_{XY}} \leq 1 \quad (6)$$

Equation (6) is the 2-simplex in normalized $\Delta H'_{P_X \cdot P_Y} \times 2MI'_{P_{XY}} \times VI'_{P_{XY}}$ space. Each joint distribution P_{XY} can be characterized by its *joint entropy fractions*, $F(P_{XY}) = [\Delta H'_{P_{XY}}, 2 * MI'_{P_{XY}}, VI'_{P_{XY}}]$, whose projection onto the plane with director vector $(1, 1, 1)$ is its *de Finetti diagram*. This diagram of the 2-simplex is an equilateral triangle whose coordinates are $F(P_{XY})$ so every bivariate distribution shows as a point in the triangle, and each zone in the triangle is indicative of the characteristics of distributions whose coordinates fall in it. This is what we call the Channel Bivariate Entropy Triangle, CBET, one of whose instances is shown below in Fig. 4.

Considering (1) and the composition of the quantities in it we can actually decompose the the equation into two *split balance equations*,

$$H_{U_X} = \Delta H_{P_X} + MI_{P_{XY}} + H_{P_{X|Y}} \quad H_{U_Y} = \Delta H_{P_Y} + MI_{P_{XY}} + H_{P_{Y|X}} \quad (7)$$

with the obvious limits. These can be each normalized by H_{U_X} , respectively H_{U_Y} , leading to the 2-simplex equations

$$1 = \Delta' H_{P_X} + MI'_{P_{XY}} + H'_{P_{X|Y}} \quad 1 = \Delta' H_{P_Y} + MI'_{P_{XY}} + H'_{P_{Y|X}} \quad (8)$$

Since these are also equations on a 2-simplex, we can actually represent the coordinates $F_X(P_{XY}) = [\Delta H'_{P_X}, MI'_{P_{XY}}, H'_{P_{X|Y}}]$ and $F_Y(P_{XY}) = [\Delta H'_{P_Y}, MI'_{P_{XY}}, H'_{P_{Y|X}}]$ in the same triangle side by side the original $F(P_{XY})$, whereby the representation seems to split in two.

1) *Application: the evaluation of multiclass classification*: This can be used to visualize the performance of supervised classifiers in a straightforward manner: consider the contingency matrix of a classifier C on a supervised classification task T given the random variable of true class labels $K \sim P_K$ and that of predicted labels $\hat{K} \sim P_{\hat{K}}$



Fig. 3. The application of CBET to multiclass classification. The classifier is trained to predict labels \hat{K} from the true emitted labels K .

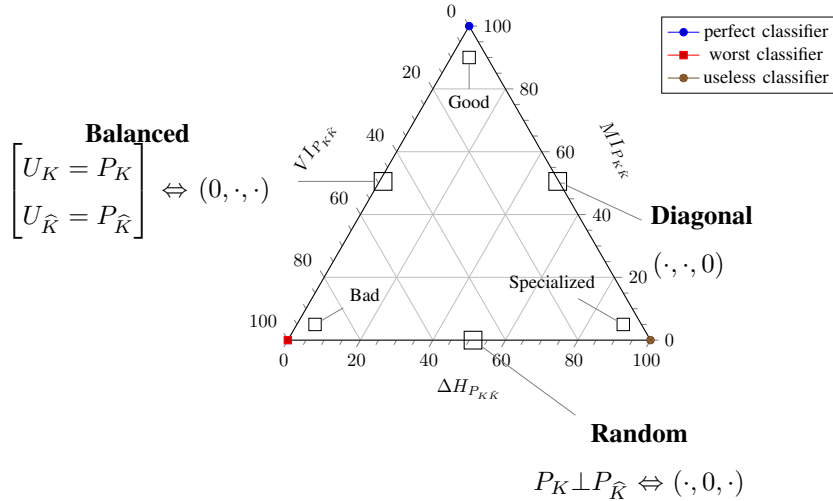


Fig. 4. **Schematic CBET as applied to supervised classifier assessment.** An actual triangle shows dots for each classifier (or its split coordinates, [see below](#)) and none of the callouts for specific types of classifiers (from [5]). The callouts situated in the center of the sides of the triangle apply to the whole side.

that now play the role of P_X and P_Y as depicted in Figure 3 . Properly normalized, this matrix can be conceived as a joint distribution $P_{K\hat{K}}$ between the random variables, so that the entropy triangle for $P_{K\hat{K}}$ produces valuable information about the actual classifier used to solve the task [1, 8], and even the theoretical limits of the task —for instance, whether it can be solved in a trustworthy manner by classification technology, and with what effectiveness.

The CBET acts, in this case, as an exploratory data analysis tool for visual assessment, as shown in Figure 4. The success of this approach in the bivariate, supervised classification case is a strong hint that the multivariate extension will likewise be useful for other machine learning tasks. See [5] for a thorough explanation of this procedure.

B. Quantities around the Multivariate Mutual Information

The main hurdle for a multivariate extension of the balance equation (1) and the CBET is the multivariate generalization of binary mutual information, since it quantifies the information transport from input to output in the bivariate case, and is also crucial for the decoupling of (1) into the split balance equations (7). For this reason, we next review the different “flavors” of information measures describing sets of more than two variables looking for these two properties.

Note that two different situations can be clearly distinguished whether the random variables

- all form part of the same set \overline{X} and we are looking at information transfer *within* this set, or
- are partitioned into two different sets \overline{X} and \overline{Y} and we are looking at information transfer *between* these sets.

An up-to-date review of multivariate information measures in both situations is [9] that follows the interesting methodological point from [10] of calling *information* those measures which involve amounts of entropy shared by multiple variables and *entropies* those that do not².

Since i-diagrams are a powerful tool to visualize the interaction of distributions in the bivariate case, we will also try to use them for sets of random variables. For multivariate generalizations of mutual information as seen in the i-diagrams, the following caveats apply:

- Their multivariate generalization is only warranted when signed measures of probability are considered, since it is well-known that some of these “areas” can be *negative*, contrary to geometric intuitions on this respect.
- We should retain the bounding rectangles that appear when considering the most entropic distributions with similar support to the ones being graphed [1]. This is the sense of the bounding rectangles in Figures 5.(a) and 5.(b).

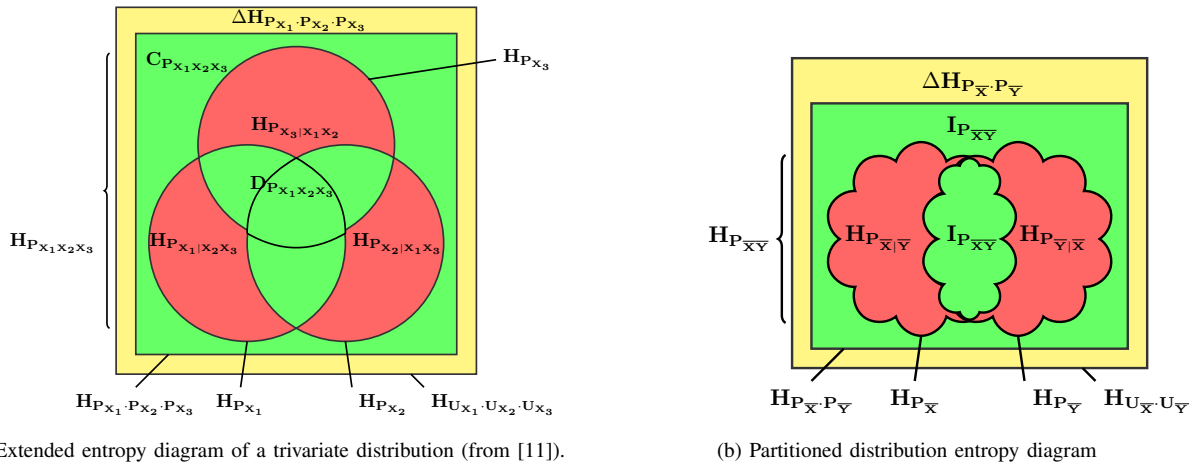


Fig. 5. (Color Online) **Extended entropy diagram of multivariate distributions for (a) a trivariate distribution (from [11]), and (b) a joint distribution where a partitioning of the variables is made evident.** The color scheme follows that of Fig. 2, to be explained in the text.

With great insight, the authors of [10] point out that some of the multivariate information measures stem from focusing in a particular property of the bivariate mutual information and generalize it to the multivariate setting. The properties in question are:

$$MI_{P_{XY}} = H_{P_X} + H_{P_Y} - H_{P_{XY}} \quad (3)$$

$$MI_{P_{XY}} = H_{P_X} - H_{P_{X|Y}} = H_{P_Y} - H_{P_{Y|X}} \quad (4)$$

$$MI_{P_{XY}} = \sum_{x,y} P_{XY}(x,y) \log \frac{P_{XY}(x,y)}{P_X(x)P_Y(y)} \quad (9)$$

Regarding the first situation of a vector of random variables $\bar{X} \sim P_{\bar{X}}$, let $\Pi_{\bar{X}} = \prod_{i=1}^n P_{X_i}$ be the (jointly) independent distribution with similar marginals to $P_{\bar{X}}$. To picture this (virtual) distribution consider Figure 5.(a) depicting an i-diagram for $\bar{X} = [X_1, X_2, X_3]$. Then $\Pi_{\bar{X}} = P_{X_1} \cdot P_{X_2} \cdot P_{X_3}$ is the inner rectangle containing both green areas. The different extensions of mutual information that concentrate on different properties are:

²Although this poses a conundrum for the entropy written as the self information $H_{P_X} = MI_{P_{XX}}$.

- the *total correlation* [12], *integration* [13] or *multiinformation* [14] is a generalization of (3), represented by the green area outside $H_{P_{\bar{X}}}$.

$$C_{P_{\bar{X}}} = H_{\Pi_{\bar{X}}} - H_{P_{\bar{X}}} \quad (10)$$

- the *dual total correlation* [15, 16] or *interaction complexity* [17] is a generalization of (4), represented by the green area inside $H_{P_{\bar{X}}}$

$$D_{P_{\bar{X}}} = H_{P_{\bar{X}}} - VI_{P_{\bar{X}}} \quad (11)$$

- the *interaction information* [18], *multivariate mutual information* [19] or *co-information* [20] is the generalization of (9), the total amount of information to which all variables contribute.

$$MI_{P_{\bar{X}}} = \sum P_{\bar{X}}(\bar{x}) \log \frac{P_{\bar{X}}(\bar{x})}{\Pi_{\bar{X}}(\bar{x})} \quad (12)$$

It is represented by the inner convex area (within the dual total correlation), but note that it may in fact be negative for $n > 2$ [21].

- the *local exogenous information* [10] or the *bound information* [22] is the addition of the total correlation and the dual total correlation

$$M_{P_{\bar{X}}} = C_{P_{\bar{X}}} + D_{P_{\bar{X}}}. \quad (13)$$

Some of these generalizations of the multivariate case were used in [11, 22] to develop a similar technique as the CBET but applied to analyzing the information content of data sources. For this purpose, it was necessary to define for every random variable a *residual entropy* $H_{P_{X_i|X_i^c}}$ —where $X_i^c = \bar{X} \setminus \{X_i\}$ —which is not explained by the information provided by the other variables. We call *residual information* [10] or *(multivariate) variation of information* [4, 22] a generalization of the same quantity in the bivariate case, the sum of these quantities across the set of random variables:

$$VI_{P_{\bar{X}}} = \sum_{i=1}^n H_{P_{X_i|X_i^c}}. \quad (14)$$

Then the variation of information can easily be seen to consist of the sum of the red areas in Figure 5.(a) and amounts to information peculiar to each variable.

The main question regarding this issue is which—if any—of these generalizations of bivariate mutual information are adequate for an analogue of the entropy balance equations and triangles. Note that all of these generalizations consider \bar{X} a homogeneous set of variables, and none consider the partitioning of the variables in \bar{X} into two subsets, for instance to distinguish between input and output ones, so the answer cannot be straightforward. This issue is clarified in Section III-A.

III. RESULTS

We are trying to find a decomposition of the entropies around characterizing a joint distribution $P_{\bar{X}\bar{Y}}$ between random vectors \bar{X} and \bar{Y} in ways analogous to those of (1) but considering multivariate input and output. Our main results are in complete analogy to those of the binary case, but with the flavour of the multivariate case.

A. The Aggregate and Split Channel Multivariate Balance Equation

Consider the modified information diagram of Figure 5.(b) highlighting entropies for some distributions around $P_{\overline{XY}}$. When we distinguish two random vectors in the set of variables \overline{X} and \overline{Y} , a proper multivariate generalization of the variation of information $VI_{P_{\overline{XY}}}$ in (5) is

$$VI_{P_{\overline{XY}}} = H_{P_{\overline{X}|\overline{Y}}} + H_{P_{\overline{Y}|\overline{X}}}. \quad (15)$$

It represents the addition of the information in \overline{X} not shared with \overline{Y} and vice-versa, as captured by the red area in Figure 5.(b). Note that since this is the addition of two entropies it is a non-negative quantity.

Next, consider $U_{\overline{XY}}$, the uniform distribution over the supports of \overline{X} and \overline{Y} , and $P_{\overline{X}} \times P_{\overline{Y}}$, the distribution created with the marginals of $P_{\overline{XY}}$ considered independent. Then, we may define a *multivariate divergence with respect to uniformity*—in analogy to (2)—as

$$\Delta H_{P_{\overline{X}} \times P_{\overline{Y}}} = H_{U_{\overline{XY}}} - H_{P_{\overline{X}} \times P_{\overline{Y}}}. \quad (16)$$

This is the yellow area in Figure 5.(b) representing the divergence of the virtual distribution $P_{\overline{X}} \times P_{\overline{Y}}$ with respect to uniformity. The virtuality comes from the fact that this distribution does not properly exist in the context being studied. Rather, it only appears in the extreme situation that the marginals of $P_{\overline{XY}}$ are independent.

Furthermore, recall that both the total entropy of the uniform distribution and the divergence from uniformity factor into individual equalities $H_{U_{\overline{X}}U_{\overline{Y}}} = H_{U_{\overline{X}}} + H_{U_{\overline{Y}}}$ —since uniform joint distributions always have independent marginals—and $H_{P_{\overline{X}} \times P_{\overline{Y}}} = H_{P_{\overline{X}}} + H_{P_{\overline{Y}}}$. Therefore (16) admits splitting as $\Delta H_{P_{\overline{X}} \times P_{\overline{Y}}} = \Delta H_{P_{\overline{X}}} + \Delta H_{P_{\overline{Y}}}$ where

$$\Delta H_{P_{\overline{X}}} = H_{U_{\overline{X}}} - H_{P_{\overline{X}}} \quad \Delta H_{P_{\overline{Y}}} = H_{U_{\overline{Y}}} - H_{P_{\overline{Y}}}. \quad (17)$$

Now, both $U_{\overline{X}}$ and $U_{\overline{Y}}$ are the most entropic distributions definable in the support of \overline{X} whence both $\Delta H_{P_{\overline{X}}}$ and $\Delta H_{P_{\overline{Y}}}$ are non-negative, as is their addition.

These generalizations are straightforward and intuitively mean what we expect them to agree with the intuitions provided by the CBET. We would like to find now a quantity that fulfills the same role as the (bivariate) mutual information.

The first property that we would like to have is for this quantity to be a “remanent information” after conditioning away any of the entropy of either partition, so we propose the following as a definition:

$$I_{P_{\overline{XY}}} = H_{P_{\overline{XY}}} - VI_{P_{\overline{XY}}} \quad (18)$$

represented by the inner green area in the i-diagram of Figure 5.(b).

This can easily be “refocused” on each of the subsets of the partition:

Lemma 1. *Let $P_{\overline{XY}}$ be a discrete joint distribution. Then*

$$H_{P_{\overline{X}}} - H_{P_{\overline{X}|\overline{Y}}} = H_{P_{\overline{Y}}} - H_{P_{\overline{Y}|\overline{X}}} = I_{P_{\overline{XY}}} \quad (19)$$

Proof. Recalling that the conditional entropies are easily related to the joint entropy by the chain rule $H_{P_{\overline{XY}}} = H_{P_{\overline{X}}} + H_{P_{\overline{Y}|\overline{X}}} = H_{P_{\overline{Y}}} + H_{P_{\overline{X}|\overline{Y}}}$, simply subtract $VI_{P_{\overline{XY}}}$. \square

This property introduces the notion that this information is *within* each of \bar{X} and \bar{Y} *independently but mutually induced*. It is easy to see that this quantity appears once again in the i-diagram:

Lemma 2. *Let $P_{\bar{X}\bar{Y}}$ be a discrete joint distribution. Then*

$$I_{P_{\bar{X}\bar{Y}}} = H_{P_{\bar{X}} \times P_{\bar{Y}}} - H_{P_{\bar{X}\bar{Y}}}. \quad (20)$$

Proof. Considering the entropy decomposition of $P_{\bar{X}} \times P_{\bar{Y}}$:

$$H_{P_{\bar{X}} \times P_{\bar{Y}}} - H_{P_{\bar{X}\bar{Y}}} = H_{P_{\bar{X}}} + H_{P_{\bar{Y}}} - (H_{P_{\bar{Y}}} + H_{P_{\bar{X}|\bar{Y}}}) = H_{P_{\bar{X}}} - H_{P_{\bar{X}|\bar{Y}}} = I_{P_{\bar{X}\bar{Y}}}$$

□

In other words, this is the quantity of information required to bind $P_{\bar{X}}$ and $P_{\bar{Y}}$; equivalently, it is the amount of information *lost* from $P_{\bar{X}} \times P_{\bar{Y}}$ to achieve the binding in $P_{\bar{X}\bar{Y}}$. Pictorially, this is the outermost green area in Fig. 5.(b), and *it must be non-negative*, since $P_{\bar{X}} \times P_{\bar{Y}}$ is more entropic than $P_{\bar{X}\bar{Y}}$. Notice that (18) and (19) are the analogues of (10) and (11), respectively, but with the flavor of (3) and (4).

This not-so-mysterious quantity must be the multivariate mutual information of $P_{\bar{X}\bar{Y}}$ as per the Kullback-Leibler divergence definition:

Lemma 3. *Let $P_{\bar{X}\bar{Y}}$ be a discrete joint distribution. Then*

$$I_{P_{\bar{X}\bar{Y}}} = \sum_{i,j} P_{\bar{X}\bar{Y}}(x_i, y_j) \log \frac{P_{\bar{X}\bar{Y}}(x_i, y_j)}{P_{\bar{X}}(x_i)P_{\bar{Y}}(y_j)} \quad (21)$$

Proof. This is an easy manipulation.

$$\begin{aligned} \sum_{i,j} P_{\bar{X}\bar{Y}}(x_i, y_j) \log \frac{P_{\bar{X}\bar{Y}}(x_i, y_j)}{P_{\bar{X}}(x_i)P_{\bar{Y}}(y_j)} &= \sum_{i,j} P_{\bar{X}\bar{Y}}(x_i, y_j) \log \frac{P_{\bar{X}|\bar{Y}=y_j}(x_i|y_j)}{P_{\bar{X}}(x_i)} = \sum_i P_{\bar{X}}(x_i) \log \frac{1}{P_{\bar{X}}(x_i)} - \\ &- \sum_j P_{\bar{Y}}(y_j) \sum_i P_{\bar{X}|\bar{Y}=y_j}(x_i|y_j) \log \frac{1}{P_{\bar{X}|\bar{Y}=y_j}(x_i|y_j)} = \\ &= H_{P_{\bar{X}}} - H_{P_{\bar{X}|\bar{Y}}} = I_{P_{\bar{X}\bar{Y}}}, \end{aligned}$$

after a step of marginalization and considering (4). □

With these relations we can state our first theorem:

Theorem 1. *Let $P_{\bar{X}\bar{Y}}$ be a discrete joint distribution. Then the following decomposition holds:*

$$\begin{aligned} H_{U_{\bar{X}} \times U_{\bar{Y}}} &= \Delta H_{P_{\bar{X}} \times P_{\bar{Y}}} + 2 * I_{P_{\bar{X}\bar{Y}}} + V I_{P_{\bar{X}\bar{Y}}} \\ 0 &\leq \Delta H_{P_{\bar{X}} \times P_{\bar{Y}}}, I_{P_{\bar{X}\bar{Y}}}, V I_{P_{\bar{X}\bar{Y}}} \leq H_{U_{\bar{X}} \times U_{\bar{Y}}} \end{aligned} \quad (22)$$

Proof. From (16) we have $H_{U_{\bar{X}} \times U_{\bar{Y}}} = \Delta H_{P_{\bar{X}} \times P_{\bar{Y}}} + H_{P_{\bar{X}} \times P_{\bar{Y}}}$ whence by introducing (18) and (20) we obtain:

$$H_{U_{\bar{X}} \times U_{\bar{Y}}} = \Delta H_{P_{\bar{X}} \times P_{\bar{Y}}} + I_{P_{\bar{X}\bar{Y}}} + H_{P_{\bar{X}\bar{Y}}} = \Delta H_{P_{\bar{X}} \times P_{\bar{Y}}} + I_{P_{\bar{X}\bar{Y}}} + I_{P_{\bar{X}\bar{Y}}} + V I_{P_{\bar{X}\bar{Y}}}. \quad (23)$$

Recall that each quantity is non-negative by (15), (16) and (21), so the only things left to be proven are the limits for each quantity in the decomposition. For that purpose, consider the following clarifying *conditions*,

- 1) \bar{X} **marginal uniformity** when $H_{P_{\bar{X}}} = H_{U_{\bar{X}}}$, \bar{Y} **marginal uniformity** when $H_{P_{\bar{Y}}} = H_{U_{\bar{Y}}}$ and **marginal uniformity** when both conditions coocur.
- 2) **Marginal independence**, when $P_{\bar{X}\bar{Y}} = P_{\bar{X}} \times P_{\bar{Y}}$.
- 3) \bar{Y} **determines** \bar{X} when $H_{P_{\bar{X}|\bar{Y}}} = 0$, \bar{X} **determines** \bar{Y} when $H_{P_{\bar{Y}|\bar{X}}} = 0$ and **mutual determination**, when both conditions hold.

Notice that these conditions are *independent of each other* and that *each fixes the value of one of the quantities in the balance*:

- for instance, in case $H_{P_{\bar{X}}} = H_{U_{\bar{X}}}$ then $\Delta H_{P_{\bar{X}}} = 0$ after (17). Similarly, if $H_{P_{\bar{Y}}} = H_{U_{\bar{Y}}}$ then $\Delta H_{P_{\bar{Y}}} = 0$. Hence when marginal uniformity holds, we have $\Delta H_{P_{\bar{X}\bar{Y}}} = 0$.
- Similarly, when marginal independence holds, we see that $I_{P_{\bar{X}|\bar{Y}}} = 0$ from (20). Otherwise stated, $H_{P_{\bar{X}|\bar{Y}}} = H_{P_{\bar{X}}}$ and $H_{P_{\bar{Y}|\bar{X}}} = H_{P_{\bar{Y}}}$.
- Finally, if mutual determination holds—that is to say the variables in either set are deterministic functions of those of the other set—by the definition of the multivariate variation of information, we have $VI_{P_{\bar{X}|\bar{Y}}} = 0$.

Therefore, these three conditions fix the lower bounds for their respectively related quantities. Likewise, the upper bounds hold when *two* of the conditions hold at the same time. This is easily seen invoking the previously found balance equation (23):

- For instance, if marginal uniformity holds, then $\Delta H_{P_{\bar{X}\bar{Y}}} = 0$. But if marginal independence also holds, then $I_{P_{\bar{X}|\bar{Y}}} = 0$ whence by (23) $VI_{P_{\bar{X}\bar{Y}}} = H_{U_{\bar{X}} \times U_{\bar{Y}}}$.
- But if both marginal uniformity and mutual determination hold, then we have $\Delta H_{P_{\bar{X}\bar{Y}}} = 0$ and $VI_{P_{\bar{X}\bar{Y}}} = 0$ so that $I_{P_{\bar{X}\bar{Y}}} = H_{U_{\bar{X}} \times U_{\bar{Y}}}$.
- Finally, if both mutual determination and marginal independence holds, then a fortiori $\Delta H_{P_{\bar{X}\bar{Y}}} = H_{U_{\bar{X}} \times U_{\bar{Y}}}$.

This concludes the proof. □

Notice how the bounds also allow an interpretation similar to that of (1). In particular, the interpretation of the conditions for actual joint distributions will be taken again in Section III-B.

The next question is whether the balance equation also admits splitting.

Theorem 2. *Let $P_{\bar{X}\bar{Y}}$ be a discrete joint distribution. Then the Channel Multivariate Entropy Balance equation can be split as:*

$$H_{U_{\bar{X}}} = \Delta H_{P_{\bar{X}}} + I_{P_{\bar{X}\bar{Y}}} + H_{P_{\bar{X}|\bar{Y}}} \quad 0 \leq \Delta H_{P_{\bar{X}}}, I_{P_{\bar{X}\bar{Y}}}, H_{P_{\bar{X}|\bar{Y}}} \leq H_{U_{\bar{X}}} \quad (24)$$

$$H_{U_{\bar{Y}}} = \Delta H_{P_{\bar{Y}}} + I_{P_{\bar{X}\bar{Y}}} + H_{P_{\bar{Y}|\bar{X}}} \quad 0 \leq \Delta H_{P_{\bar{Y}}}, I_{P_{\bar{X}\bar{Y}}}, H_{P_{\bar{Y}|\bar{X}}} \leq H_{U_{\bar{Y}}} \quad (25)$$

Proof. We prove (24): the proof of (25) is similar *mutatis mutandis*.

In a similar way as for (22), we have that $H_{U_{\bar{X}}} = \Delta H_{P_{\bar{X}}} + H_{P_{\bar{X}}}$. By introducing the value of $H_{P_{\bar{X}}}$ from (19) we obtain the decomposition of $H_{U_{\bar{X}}}$ of (24).

These quantities are non-negative, as mentioned. Next consider the \bar{X} marginal uniformity condition applied to the input vector introduced in the proof of Theorem 1. Clearly, $\Delta H_{\bar{X}} = 0$. Marginal independence, again, is the

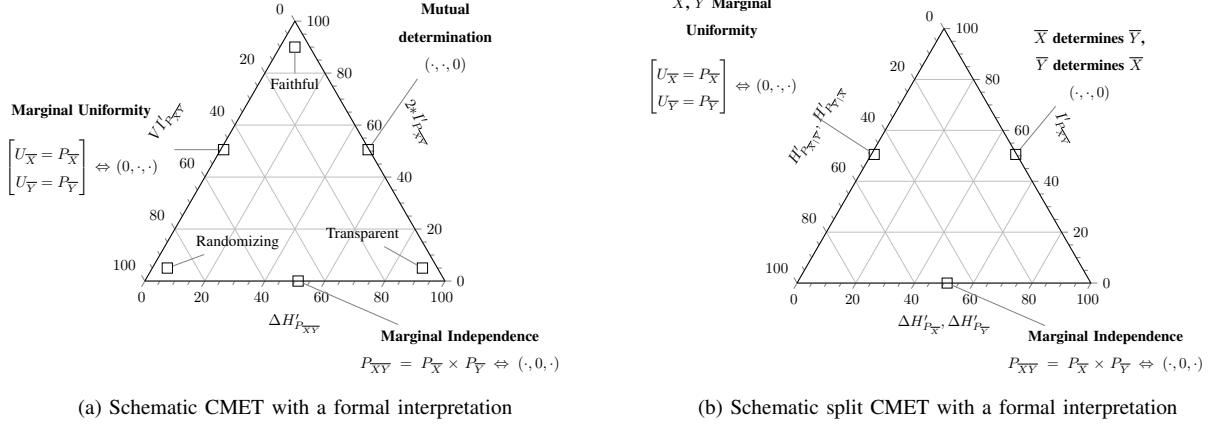


Fig. 6. **Schematic Channel Multivariate Entropy Triangles (CMET) showing interpretable zones and extreme cases using formal conditions.** The annotations on the center of each side are meant to hold for that whole side, those for the vertices are meant to hold in their immediate neighborhood too.

condition so that $I_{\overline{X}\overline{Y}} = 0$. Finally, if \overline{Y} determines \overline{X} then $H_{P_{\overline{X}|\overline{Y}}} = 0$. These conditions individually provide the lower bounds on each quantity.

On the other hand, when we put together any two of these conditions, we obtain the upper bound for the unspecified variable: so, if $\Delta H_{P_{\overline{X}}} = 0$ and $I_{P_{\overline{X}\overline{Y}}} = 0$ then $H_{P_{\overline{X}|\overline{Y}}} = H_{P_{\overline{X}}} = H_{U_{\overline{X}}}$. Also, if $I_{P_{\overline{X}\overline{Y}}} = 0$ and $H_{P_{\overline{X}|\overline{Y}}} = 0$, then $H_{P_{\overline{X}}} = H_{P_{\overline{X}|\overline{Y}}} = 0$ and $\Delta H_{P_{\overline{X}}} = H_{U_{\overline{X}}} - 0$. Finally, if $H_{P_{\overline{X}|\overline{Y}}} = 0$ and $\Delta H_{P_{\overline{X}}} = 0$, then $I_{P_{\overline{X}\overline{Y}}} = H_{P_{\overline{X}}} - H_{P_{\overline{X}|\overline{Y}}} = H_{U_{\overline{X}}} - 0$. \square

B. Visualizations: From i -Diagrams to Entropy Triangles

1) *The Channel Multivariate Entropy triangle:* As in the case of the CBET, we need the equation of a simplex to represent the information balance of a multivariate transformation. For that purpose, as in (6) we may normalize by the overall entropy $H_{U_{\overline{X}} \times U_{\overline{Y}}}$ to obtain the equation of the 2-simplex in multivariate entropic space,

$$1 = \Delta' H_{P_{\overline{X}} \times P_{\overline{Y}}} + 2 * I'_{P_{\overline{X}\overline{Y}}} + V I'_{P_{\overline{X}\overline{Y}}} \quad (26)$$

$$0 \leq \Delta' H_{P_{\overline{X}} \times P_{\overline{Y}}}, I'_{P_{\overline{X}\overline{Y}}}, V I'_{P_{\overline{X}\overline{Y}}} \leq 1.$$

The de Finetti diagram of this equation then provides the aggregated *Channel Multivariate Entropy Triangle, CMET*.

A *formal* graphical assessment of multivariate joint distribution with the CMET is fairly simple using the schematic in Fig. 6.(a) and the conditions of Theorem 1:

- The lower side of the triangle with $I'_{P_{\overline{X}\overline{Y}}} = 0$, affected of *marginal independence* $P_{\overline{X}\overline{Y}} = P_{\overline{X}} \times P_{\overline{Y}}$, is the locus of partitioned joint distributions who do not share information between the two blocks \overline{X} and \overline{Y} .
- The right side of the triangle with $V I'_{P_{\overline{X}\overline{Y}}} = 0$, described with *mutual determination* $H'_{P_{\overline{X}|\overline{Y}}} = 0 = H'_{P_{\overline{Y}|\overline{X}}}$, is the locus of partitioned joint distributions whose groups do not carry supplementary information to that provided by the other group.

- The left sidewith $\Delta H'_{P_{\overline{X}\overline{Y}}} = 0$, describing distributions with *uniform marginals* $P_{\overline{X}} = U_{\overline{X}}$ and $P_{\overline{Y}} = U_{\overline{Y}}$, is the locus of partitioned joint distributions that offer as much potential information for transformations as possible.

Based on these characterizations we can attach interpretations to other regions of the CMET:

- If we want a transformation from \overline{X} to \overline{Y} to be *faithful*, then we want to maximize the information used for mutual determination $I'_{P_{\overline{X}\overline{Y}}} \rightarrow 1$, equivalently, minimize at the same time the divergence from uniformity $\Delta H'_{P_{\overline{X}\overline{Y}}} \rightarrow 0$ and the information that only pertains to each of the blocks in the partition $VI'_{P_{\overline{X}\overline{Y}}} \rightarrow 0$. So the coordinates of a faithful partitioned joint distribution will lay close to the apex of the triangle.
- However, if the coordinates of a distribution lay close to the left vertex $VI'_{P_{\overline{X}\overline{Y}}} \rightarrow 1$, then it shows marginal uniformity $\Delta H'_{P_{\overline{X}\overline{Y}}} \rightarrow 0$ but shares little or no information between the blocks $I'_{P_{\overline{X}\overline{Y}}} \rightarrow 0$, hence it must be a *randomizing* transformation.
- Distributions whose coordinates lay close to the right vertex $\Delta H'_{P_{\overline{X}\overline{Y}}} \rightarrow 1$ are essentially deterministic and in that sense carry no information $I'_{P_{\overline{X}\overline{Y}}} \rightarrow 0, VI'_{P_{\overline{X}\overline{Y}}} \rightarrow 0$. Indeed in this instance there does not seem to exist a transformation, whence we call them *rigid*.

These qualities are annotated on the vertices of the schematic CMET of Fig. 6.(a). Note that different applications may call for partitioned distributions with different qualities and the one used above is pertinent when the partitioned joint distributions models a transformation of \overline{X} into \overline{Y} or vice-versa.

2) *Normalized Split Channel Multivariate Balance Equations:* With a normalization similar to that from (7) to (8), (24) and (25) naturally lead to 2-simplex equations normalizing by $H_{U_{\overline{X}}}$ and $H_{U_{\overline{Y}}}$, respectively

$$1 = \Delta' H_{P_{\overline{X}}} + I'_{P_{\overline{X}\overline{Y}}} + H'_{P_{\overline{X}|\overline{Y}}} \quad (27)$$

$$0 \leq \Delta' H_{P_{\overline{X}}}, I'_{P_{\overline{X}\overline{Y}}}, H'_{P_{\overline{X}|\overline{Y}}} \leq 1$$

$$1 = \Delta' H_{P_{\overline{Y}}} + I'_{P_{\overline{X}\overline{Y}}} + H'_{P_{\overline{Y}|\overline{X}}} \quad (28)$$

$$0 \leq \Delta' H_{P_{\overline{Y}}}, I'_{P_{\overline{X}\overline{Y}}}, H'_{P_{\overline{Y}|\overline{X}}} \leq 1$$

Note that the quantities $\Delta H'_{P_{\overline{X}}}$ and $\Delta H'_{P_{\overline{Y}}}$ have been independently motivated and named *redundancies* [23, § 2.4].

These are actually two different representations for each of the two blocks in the partitioned joint distribution. Using the fact that they share one coordinate— $I'_{P_{\overline{X}\overline{Y}}}$ —and the rest are analogues— $\Delta' H_{P_{\overline{X}}}$ and $\Delta' H_{P_{\overline{Y}}}$ on one side, and $H'_{P_{\overline{X}|\overline{Y}}}$ and $H'_{P_{\overline{Y}|\overline{X}}}$ on the other—we can represent both equations *at the same time* in a single de Finetti diagram. We call this representation the *split Channel Multivariate Entropy Triangle*, an schema of which can be seen in Fig. 6.(b). The qualifying “split” then refers to the fact that each partitioned joint distribution appears as *two points* in the diagram. Note the double annotation in the left and bottom coordinates implying that there are *two* different diagrams overlapping.

Conventionally, the point referring to the \overline{X} block described by (27) is represented with a cross, while the point referring to the \overline{Y} block described by (28) is represented with a circle as will be noted in Figure 8.

The formal interpretation of this split diagram with the conditions of Theorem 1 follows that of the aggregated CMET but considering only one block at a time, for instance, for \overline{X} :

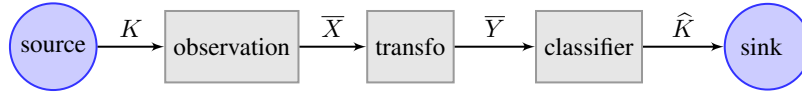


Fig. 7. Conceptual representation as a communication channel of a supervised classification task (from [11])

- The lower side of the triangle is interpreted as before.
- The right side of the triangle is the locus of the partitioned joint distribution whose \overline{X} block is completely determined by the \overline{Y} block, that is, $H'_{P_{\overline{X}|\overline{Y}}} = 0$.
- The left side of the triangle $\Delta H'_{P_{\overline{X}}} = 0$ is the locus of those partitioned joint distributions whose \overline{X} marginal is uniform $P_{\overline{X}} = U_{\overline{X}}$.

The interpretation is analogue for \overline{Y} *mutatis mutandis*.

The purpose of this representation is to investigate the formal conditions separately on each block. However, for this split representation we have to take into consideration that the normalizations may not be the same, that is $H_{P_{\overline{X}}}$ and $H_{P_{\overline{Y}}}$ are, in general, different.

A full example of the interpretation of both types of diagrams, the CMET and the split CMET is provided in the next Section in the context of an application.

C. Example application: data transformation analysis

In this Section we present an application of the results obtained above to the analysis of the information transmission through specific instances of data transformation procedures. Data transformation is an ubiquitous step in machine learning whereby available data—e.g. the observations in the dataset \overline{X} —gets transformed into another data with “better” characteristics—the transformed feature vectors \overline{Y} . These characteristics may be representational power, independence between individual dimensions, etc. Note, for example, that the feature mappings that take place in each of the layers an Artificial Neural Network are an example of learned data transformations.

Consider the conceptual schema in Figure 7 describing a supervised classification task where \overline{X} represents the random vector of observations or features, K is the random variable of the true class, \hat{K} represents the random variable of the guessed class and \overline{Y} represents a random vector of transformed observations. The latter are the input to the actual classifier so its choice is typically dictated by the chosen technology or algorithm for the classifier.

An extended practice in supervised classification is to explore different transformations of the observations and then evaluate such different approaches on different classifiers for a particular task [24]. Instead of this “in the loop” evaluation—that conflates the evaluation of the transformation and the classification—we will use the CMET to evaluate *only* the transformation. In particular we will evaluate the use of Principal Component Analysis PCA [25] and Independent Component Analysis ICA [26] which have, purportedly, different aims.

PCA is a staple technique in statistical data analysis and machine learning based in the Singular Value Decomposition of the data matrix to obtain projections along the singular vectors that account for its variance in decreasing

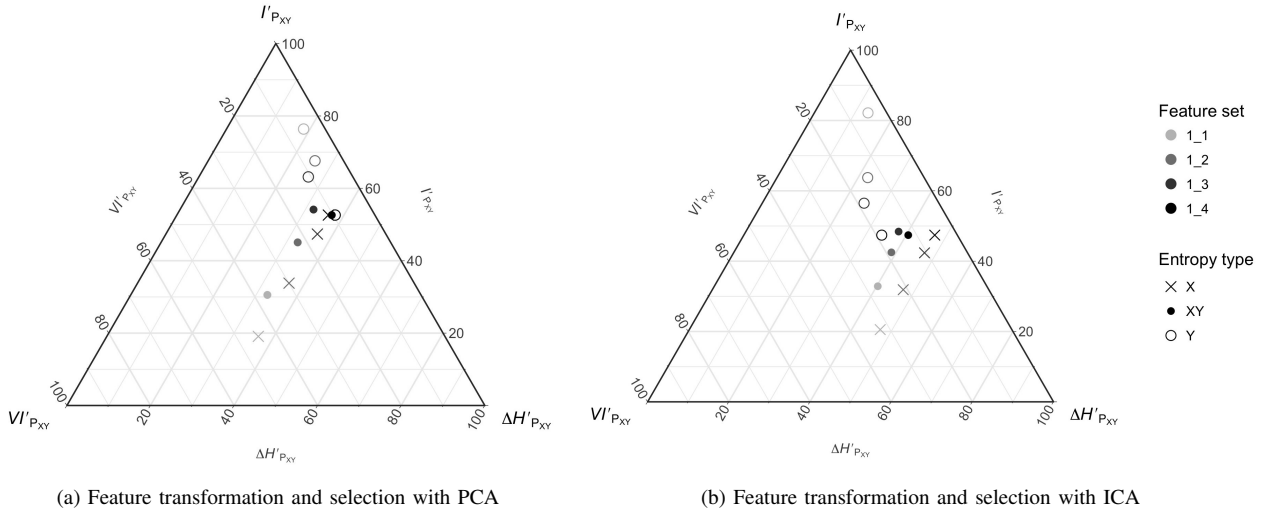


Fig. 8. Exploration of feature transformation and selection with PCA (left) and ICA (right) on `iris` when selecting the first n ranked features as obtained for each method. PCA has the potential for more a higher information transfer in this instance.

amount. While PCA aims at orthogonalization of the projections, ICA finds the projections, also known as *factors*, by maximizing their statistical independence, in our example by minimizing their mutual information [27].

The implementation used in our examples are those of the `stats` (v. 3.3.3) and `ica` (v. 1.0-1) R packages publicly available. The entropy diagrams and calculations were carried out with the open-source `entropies` experimental R package that provides an implementation of the present framework [28].

Figure 8.(a) presents the results of the PCA transformation on the logarithm of the features of Anderson’s `iris`. Crosses represent \bar{X} using (27) while circles represent \bar{Y}_i using (28) and filled circles the aggregate representation of (26). We represent several possible features sets \bar{Y}_i as output where each is obtained selecting the first i features in the ranking provided by PCA. Since `iris` has four features we can make four different feature sets of 1 to i features. For instance \bar{Y}_2 represents choosing features 1 – 2. The figure then explores how the information in the whole database \bar{X} is transported to different, nested candidate feature sets \bar{Y}_i as per the PCA recipe: choose as many ranked features as required to account for the variance of the data.

We first notice that all the points for \bar{X} lie on a line parallel to the left side of the triangle and their average transmitted information is increasing, parallel to a decrease in remanent information. Indeed, the redundancy $\Delta H'_{\bar{X}} = \frac{\Delta H_{\bar{X}}}{H_{U_{\bar{X}}}}$ is the same regardless of the choice of \bar{Y}_i . The monotonic increase with the number of features selected i in *average transmitted information* $I'_{P_{\bar{X}\bar{Y}_i}} = \frac{I_{P_{\bar{X}\bar{Y}_i}}}{H_{U_{\bar{X}}}}$ in (27) corresponds to the monotonic increase in absolute transmitted information $I_{P_{\bar{X}\bar{Y}_i}}$: for a given input set of features \bar{X} , the more output features are selected, the higher the mutual information between input and output. This is the basis of the effectiveness of the feature-selection procedure.

Regarding the points for \bar{Y}_i , note that the *absolute* transmitted information also appears in the *average* (with respect to \bar{Y}_i) transmitted information as $I'_{P_{\bar{X}\bar{Y}_i}} = \frac{I_{P_{\bar{X}\bar{Y}_i}}}{H_{U_{\bar{Y}_i}}}$ in (28). While $I_{P_{\bar{X}\bar{Y}_i}}$ increases with i , as mentioned, we actually see a monotonic *decrease* in $I'_{P_{\bar{X}\bar{Y}_i}}$. The reason for this is the rapidly increasing value of the denominator

$H_{U_{\bar{Y}_i}}$ as we select more and more features.

Finally, notice how these two tendencies are conflated in the aggregate plot for the \overline{XY}_i that shows a lopsided, inverted U pattern, peaking before i reaches its maximum. This suggests that if we balance aggregated transmitted information against number of features selected—the complexity of the representation—in the search for a *faithful* representation, the average transmitted information is the quantity to optimize, that is, the *mutual determination* between the two feature sets.

Figure 8.(b) presents similar results on the ICA transformation on the logarithm of the features of Anderson’s *iris* with the same glyph convention as for PCA, but the ranking resulting from the ICA method. Note that the transformed features produce by PCA and ICA are, in principle, very different, but the phenomena described for PCA are also apparent here: an increase in *aggregate* transmitted information, checked by the increase of the denominator represented by $H_{U_{\bar{Y}_i}}$ which implies a decreasing *average* transmitted information for \bar{Y}_i .

With the present framework the question of which transformation is “better” for this dataset can be given content and rephrased as *which transformation transmits more information on average on this dataset*, and also, importantly, *whether the aggregate information available in the dataset is being transmitted* by either of these methods. This is explored in Figure 9 where, for reference, we have included a point for the (deterministic) transformation of the logarithm, the cross, giving an idea of what an information-lossless transformation can achieve that consequently appears on the right side of the triangle implying *mutual determination* between \bar{X} and \bar{Y} . The first interesting observation is that neither technique is transmitting all of the information in the database, which can be gleaned from the fact that both feature sets “1_4”—when all the features available have been selected—are well below the star. This clearly follows the data processing inequality, but is still surprising since transformations like ICA and PCA are extensively used and considered to work well in practice. In this instance it can only be explained by the dimensionality reduction achieved.

Actually, the observations in the CMET actually suggest that the best we can aim is at *maintaining* the average transmitted information per feature and this can be done by selecting up to two features in the case of ICA, and up to three in the case of PCA. Referring back to Figure 8 we can see that this leaves almost half of the aggregate information out of the transformed features.

D. Discussion

The development of the multivariate case is quite parallel to the bivariate case. An important point to realize is that the multivariate mutual information between two different random vectors $I_{P_{\overline{XY}}}$ is the proper generalization for the usual mutual information $I_{P_{XY}}$ in the bivariate case, rather than the more complex alternatives used in multivariate sources [11]. Indeed properties (18) and (20) are crucial in transporting the structure and intuitions built from the bivariate channel entropy triangle to the multivariate one, of which the former is a proper instance. This was not the case with stochastic sources of information [11].

The crucial quantities in the balance equation and the triangle have been independently motivated by other works. First, multivariate mutual information is fundamental in Information Theory, and we already mentioned the redundancy ΔH_{P_X} [23]. We also mentioned the input-entropy normalized $I'_{P_{\overline{XY}}}$ used as a standalone assessment

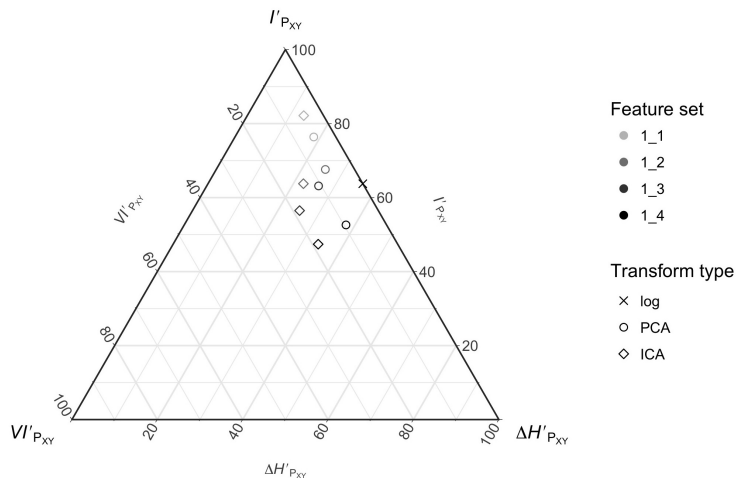


Fig. 9. **Comparison of PCA and ICA as data transformations using the CMET.** Both seem similar in what they accomplish, if ICA does it more succinctly in this instance.

measure in intrusion detection [29]. Perhaps the least known quantity in the paper was the variation of information. Despite being inspired by the concept proposed by Meila [4], to the best of our knowledge it is completely new in the multivariate setting. However, the underlying concepts of conditional or remanent entropies have proved time and again their utility. All of the above is indirect proof that the quantities studied in this paper are significant, and the existence of a balance equation binding them together, a welcome surprise.

The normalizations involved in (6) and (26)—respectively, (8), (27) and (28)—are similar conceptually: to divide by the logarithm of the total size of the domains involved whether it is the size of $X \times Y$ or that of $\bar{X} \times \bar{Y}$. Notice, first, that this is the same as taking the logarithm base these sizes in the non-normalized equations. The resulting units would not be bits for the multivariate case proper, since the size of \bar{X} or \bar{Y} is at least $2 \times 2 = 4$. But since the entropy triangles represent compositions, which are inherently dimensionless, this allows us to represent many different, and otherwise incomparable systems, e.g. univariate and multivariate ones. Second, this type of normalization allows for an interpretation of the extension of these measures to the continuous case as a limit in the process of equipartitioning a compact support, as done, for instance, for the Rényi entropy in [30, § 3] which is known to be a generalization of Shannon’s. There are hopes, then for a continuous version of the balance equations leading to an entropy diagram representation.

Finally, note that the application presented in Section III-C above, although principled in the framework presented here, is not a systematic approach to analyzing transformations. For that, a wider selection of data transformation approaches and many more datasets should be assessed. Furthermore, the feature selection process used the “filter” approach which for supervised tasks seems suboptimal. Future work will address this issue as well as how the technique developed here relates to the end-to-end assessment presented in [5] and the source characterization technique of [11].

IV. CONCLUSION

We have provided the theory and some tools on how to calculate and visualize the entropies and information transferred from a multivariate source of information \bar{X} to a multivariate sink of information \bar{Y} related by a joint distribution $P_{\bar{X}\bar{Y}}$. For that purpose we have generalized a similar previous theory and visualization tools for bivariate sources greatly extending the applicability of the results.

To carry out this extension we had to look into the multivariate version of mutual information. First we obtained a balance equation of Shannon-type entropies involving the multivariate mutual information $I_{P_{\bar{X}\bar{Y}}}$, the redundancies of the random vectors $\Delta H_{P_{\bar{X}}}$ and $\Delta H_{P_{\bar{Y}}}$ and the variation of information $VI_{P_{\bar{X}\bar{Y}}}$. When properly normalized, this leads to a visualization diagram in the form of a de Finetti diagram to represent instances of joint distributions.

Finally we tested the technique in the problem of quantifying the transference of information in data transformations, an ubiquitous procedure in data analysis. We believe this is a fruitful approach e.g. for the assessment of learning systems and foresee a bevy of applications to come.

ACKNOWLEDGMENT

CPM & FVA have been partially supported by the Spanish Government-MinECo projects TEC2014-53390-P and TEC2014-61729-EXP in this research.

REFERENCES

- [1] F. J. Valverde-Albacete and C. Peláez-Moreno, “Two information-theoretic tools to assess the performance of multi-class classifiers,” *Pattern Recognition Letters*, vol. 31, no. 12, pp. 1665–1671, 2010.
- [2] C. E. Shannon, “A mathematical theory of Communication,” *The Bell System Technical Journal*, vol. XXVII, no. 3, pp. 379–423, Jul. 1948.
- [3] —, “A mathematical theory of communication,” *The Bell System Technical Journal*, vol. XXVII, no. 3, pp. 623–656, Jul. 1948.
- [4] M. Meila, “Comparing clusterings—an information based distance,” *Journal of Multivariate Analysis*, vol. 28, pp. 875–893, 2007.
- [5] F. J. Valverde-Albacete and C. Peláez-Moreno, “100% classification accuracy considered harmful: the normalized information transfer factor explains the accuracy paradox,” *PLOS ONE*, pp. 1–10, january 2014.
- [6] R. Yeung, “A new outlook on Shannon’s information measures,” *IEEE Transactions on Information Theory*, vol. 37, no. 3, pp. 466–474, 1991.
- [7] F. M. Reza, *An introduction to information theory*, ser. McGraw-Hill Electrical and Electronic Engineering Series. McGraw-Hill Book Co., Inc., New York-Toronto-London, 1961.
- [8] F. J. Valverde-Albacete, J. C. de Albornoz, and C. Peláez-Moreno, “A proposal for new evaluation metrics and result visualization technique for sentiment analysis tasks,” in *Information Access Evaluation. Multilinguality, Multimodality and Visualization. Proceedings of CLEF 2013*, ser. LNCS, P. Forner, henning Müller, R. Paredes, P. Rosso, and B. Stein, Eds., vol. 8138. Springer, 2013, pp. 41–52.

- [9] N. Timme, W. Alford, B. Flecker, and J. M. Beggs, “Synergy, redundancy, and multivariate information measures: an experimentalist’s perspective,” *Journal of Computational Neuroscience*, vol. 36, no. 2, pp. 119–140, 2014.
- [10] R. G. James, C. J. Ellison, and J. P. Crutchfield, “Anatomy of a bit: Information in a time series observation.” *Chaos*, vol. 21, no. 3, pp. 037 109–037 109, Aug. 2011.
- [11] F. J. Valverde-Albacete and C. Peláez-Moreno, “The evaluation of data sources using multivariate entropy tools,” *Expert Systems with Applications*, vol. 78, pp. 145–157, 2017.
- [12] S. Watanabe, “Information theoretical analysis of multivariate correlation,” *International Business Machines Corporation. Journal of Research and Development*, vol. 4, no. 1, pp. 66–82, 1960.
- [13] G. Tononi, O. Sporns, and G. M. Edelman, “A measure for brain complexity: relating functional segregation and integration in the nervous system.” *Proceedings of the National Academy of Sciences of the United States of America*, vol. 91, no. 11, pp. 5033–5037, May 1994.
- [14] M. Studený and J. Vejnarová, “The Multiinformation Function as a Tool for Measuring Stochastic Dependence,” in *Learning in Graphical Models*. Dordrecht: Springer Netherlands, 1998, pp. 261–297.
- [15] T. S. Han, “Nonnegative entropy measures of multivariate symmetric correlations,” *Information and Control*, vol. 36, no. 2, pp. 133–156, Feb. 1978.
- [16] S. A. Abdallah and M. D. Plumbley, “A measure of statistical complexity based on predictive information with application to finite spin systems,” *Physics Letters A*, vol. 376, no. 4, pp. 275–281, 2012.
- [17] G. Tononi, “Complexity and coherency: integrating information in the brain,” *Trends in Cognitive Sciences*, vol. 2, no. 12, pp. 474–484, Dec. 1998.
- [18] W. J. McGill, “Multivariate information transmission,” *Psychometrika*, vol. 19, no. 2, pp. 97–116, 1954.
- [19] T. Sun Han, “Multiple mutual informations and multiple interactions in frequency data,” *Information and Control*, vol. 46, no. 1, pp. 26–45, Jul. 1980.
- [20] A. Bell, “The co-information lattice,” in *Proceedings of the Fifth International Workshop on Independent Component Analysis and Blind Signal Separation*, N. Murata, S.-i. Amari, A. Cichocki, and S. Makino, Eds., Jan. 2003.
- [21] S. A. Abdallah and M. D. Plumbley, “Predictive Information, Multiinformation and Binding Information,” Queen Mary, University of London, Tech. Rep. C4DM-TR10-10, Dec. 2010.
- [22] F. J. Valverde Albacete and C. Peláez-Moreno, “The multivariate entropy triangle and applications,” in *Hybrid Artificial Intelligence Systems (HAIS 2016), Proceedings*. Seville (Spain): Springer, April 2016, pp. 1–12.
- [23] D. J. C. MacKay, *Information Theory, Inference and Learning Algorithms*. Cambridge University Press, Sep. 2003.
- [24] I. H. Witten, F. Eibe, and M. A. Hall, *Data mining. Practical machine learning tools and techniques*, 3rd ed. Morgan Kaufmann, 2011.
- [25] K. Pearson, “On Lines and Planes of Closest Fit to Systems of Points in Space,” *Philosophical Magazine*, no. 11, pp. 559–572, 1901.
- [26] A. J. Bell and T. J. Sejnowski, “An Information-Maximization Approach to Blind Separation and Blind

- Deconvolution,” *Neural Computation*, vol. 7, no. 6, pp. 1129–1159, Nov. 1995.
- [27] K. P. Murphy, *Machine Learning. A Probabilistic Perspective*. MIT Press, 2012.
- [28] F. J. Valverde-Albacete and C. Peláez-Moreno, “entropies – plotting ternary entropy diagrams for joint distributions, contingency matrices, etc.”
- [29] G. Gu, P. Fogla, D. Dagon, W. Lee, and B. Skorić, “Measuring intrusion detection capability: An information-theoretic approach,” in *Proceedings of the 2006 ACM Symposium on Information, Computer and Communications Security*, ser. ASIACCS '06. New York, NY, USA: ACM, 2006, pp. 90–101. [Online]. Available: <http://doi.acm.org/10.1145/1128817.1128834>
- [30] P. Jizba and T. Arimitsu, “The world according to Rényi: thermodynamics of multifractal systems,” *Annals of Physics*, vol. 312, no. 1, pp. 17–59, Jul. 2004.